OXYGEN SITES AT MOLYBDENA AND VANADIA SURFACES: ENERGETICS OF THE RE-OXIDATION PROCESS

Renata TOKARZ-SOBIERAJ[a1], Robert GRYBOS[a2], Małgorzata WITKO[a3,*] and Klaus HERMANN[b]

[a] *Institute of Catalysis and Surface Chemistry, Polish Academy of Sciences, ul. Niezapominajek 8, 30 239 Krakow, Poland; e-mail: [1] nctokarz@cyf-kr.edu.pl, [2] ncgrybos@cyf-kr.edu.pl, [3] ncwitko@cyf-kr.edu.pl*

[b] *Fritz-Haber-Institut der Max-Planck-Gesellschaft, Faradayweg 4–6, 14 195 Berlin, Germany; e-mail: hermann@fhi-berlin.mpg.de*

Received June 24, 2003
Accepted October 20, 2003

To Rudolf on his 75th Anniversary with very best wishes and warmest memories of the days he was coming to Poland to watch Wajda's Men of Marble and Iron.

Małgorzata

In oxidation reactions proceeding in accordance with the Mars–van Krevelen mechanism lattice oxygen plays the role of an oxidizing agent. Surface vacancies created by incorporation of lattice oxygen into reacting molecules are filled in a subsequent step by gaseous oxygen or, if not enough oxygen is present in the reaction environment, by oxygen diffusion from the bulk. During this process, a very active, electrophilic surface oxygen species may be formed. In effect, total combustion takes place decreasing the selectivity for partial oxidation products. The thermodynamic aspect of this effect (neglecting reaction barriers) is demonstrated for molybdenum trioxide and vanadium pentoxide. On the catalytically most interesting surfaces, MoO_3(010) and V_2O_5(010), three structurally different types of oxygen sites are present which exhibit different properties with respect to vacancy creation and annihilation. Re-oxidation of the catalyst by gaseous oxygen leads to oxygen molecules adsorbed in vacancies, preferably in an orientation parallel to the surface. Adsorption of the oxygen molecule in the vacancy leads to its activation followed by easy release of a neutral oxygen atom, which can be identified as the electrophilic species responsible for total combustion.

Keywords: Molybdenum and vanadium oxides; Active sites; Surface re-oxidation; DFT calculations; Heterogeneous catalysis; Reaction mechanism; Oxidations.

Understanding the mechanism of any catalytic reaction requires detailed knowledge of the physical and chemical properties of the catalyst surface, a characterization of the transition complexes formed at the surface, and a description of all elementary steps of the reaction. The basic task is to study

the catalyst surface since it is responsible for the interaction and binding with adsorbate(s), bond changes, chemical reaction and product desorption processes. In catalytic oxidation the dynamics of the surface following from its reduction (by formation of surface oxygen vacancies) and re-oxidation (filling of vacancies by gaseous oxygen or diffusion of bulk oxygen) is of primary importance.

There are two parallel and complementary tools, which provide information on the atomic and electronic structure of the surface: sophisticated surface experimental techniques and advanced theoretical methods based on quantum chemistry and/or solid-state physics. Nowadays, theoretical, in particular computational, investigations are constantly gaining importance, becoming an indispensable instrument in researcher's toolbox. In particular, density functional theory (DFT) is now fully matured and reliable after recognizing its limitations. These computational *ab initio* methods ("virtual experiments") prove to be very cost-effective and provide insight into the investigated system that cannot be matched by any empirical method.

Most of the basic research in the field of catalysis is focused on the rate-limiting step in the pursuit of maximum activity. However, when considering the selective action of the catalyst other reaction steps may become important. Good examples are transition metal oxides used for selective oxidation of hydrocarbons[1]. Such reactions proceed usually according to the Mars–van Krevelen mechanism in which surface oxygen takes part in the reaction and gas phase oxygen is used only to replenish oxygen vacancies created by the process. During this redox cycle many different oxygen species may be present at or near the surface:

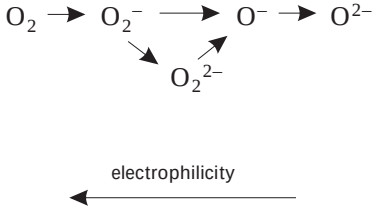

It is known that nucleophilic oxygen species leads to selective oxidation products while electrophilic results in total combustion[2–4]. This shows that a proper discussion of catalyst selectivity is impossible without considering the full reaction cycle.

Two common transition metal oxides, forming the basis for many commercial catalysts used in selective oxidation processes, are chosen in this work, molybdenum trioxide MoO_3 (refs[5–7]), and vanadium pentoxide, V_2O_5 (refs[1,6,8]). Among several factors responsible for their catalytic activity one should mention the different reactivity of different oxygen sites, the mobility of surface/lattice oxygen, and the existence of Lewis acid-base sites. In a typical catalyst the oxide surface undergoes reduction where oxygen vacancies are formed. The parent structure is transformed first into a mixed-valence oxide and then into the lower-valence oxide (for example $V_2O_5 \rightarrow (V_4O_9, V_6O_{13}) \rightarrow VO_2 \rightarrow V_2O_3$ or $MoO_3 \rightarrow (Mo_4O_{11}, Mo_{18}O_{52}) \rightarrow MoO_2$). At any step the reduction can be stopped and reversed by gaseous oxygen, which fills the vacancies and leads to re-oxidation of the surface. The combination of re-oxidation and structure transformation is a very complicated process. The present work focuses only on one component, the filling of vacancies formed at the surfaces of the highest-valence oxides (MoO_3 and V_2O_5) by molecular oxygen.

GEOMETRIC STRUCTURE OF MoO_3 AND V_2O_5

Both oxides, molybdenum trioxide[9,10] and vanadium pentoxide[11,12] crystallize in an orthorhombic layer-type lattice (Fig. 1). The crystallographic structure of molybdenum oxide (VI) may be viewed as a system of weakly bonded bilayers parallel to the (010) netplane. Each bilayer consists of two interleaved planes of corner-linked distorted MoO_6 octahedra (building units) where the octahedra of adjacent planes share edges. Each building

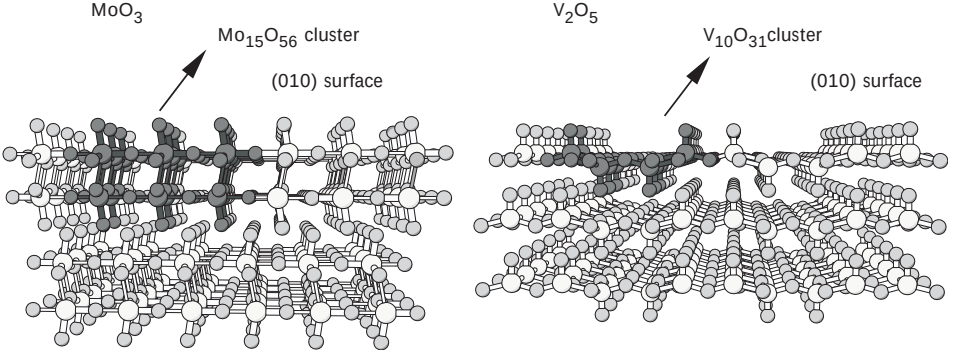

FIG. 1
Geometric structures of the (010)-oriented single crystal surface of orthorhombic MoO_3 and V_2O_5. Mo/V and oxygen centers are shown by large and small balls. The $Mo_{15}O_{56}$ and $V_{10}O_{31}$ surface sections used in cluster model calculations are indicated by shaded balls

unit is characterized by two shorter (1.67 and 1.73 Å) and four longer (between 1.94 and 2.33 Å) Mo–O bonds where the largest value, 2.33 Å, refers to the inter-planar distance within the bilayer. In V_2O_5 the building unit consists also of distorted octahedral VO_6 with one short bond at 1.59 Å, four bonds in the range between 1.78 and 2.02 Å, and one very long bond (2.79 Å), determining the layered structure. As a consequence, the catalytically active (010) surface of V_2O_5 can be characterized as containing edge- and corner-sharing distorted VO_5 square pyramids (see Fig. 1).

The variety of metal–oxygen distances in the present systems results in differently coordinated surface oxygen ions and has a large impact on catalytic properties. Both molybdenum and vanadium oxides contain oxygen coordinated to one, O(1), to two, O(2), and to three metal centers, O(3) (Fig. 2). In both systems, singly bonded O(1), molybdenyl and vanadyl, binds to the metal almost parallel to [010] direction at distances of 1.67 and 1.58 Å, respectively. In the case of bridging oxygen the definition of doubly coordinated oxygen is not completely clear. In MoO_3 the O(2) species is placed asymmetrically and is coordinated to molybdenum by one short (1.73 Å) strong bond and one long (2.25 Å) very weak bond. In effect, this bridging O(2) in MoO_3 possesses many properties of singly bonded oxygen O(1) and may be viewed as a second molybdenyl center, located along the [100] direction. In V_2O_5 the O(2) species bridges two metal centers symmetrically with two equal V–O bonds (1.88 Å) and, hence, the interaction of O(2) with its two nearest vanadium neighbors is identical. The other type of bridging oxygen, O(3), shows also differences in its geometrical environment in MoO_3 compared with V_2O_5. In MoO_3 the O(3) is placed symmetri-

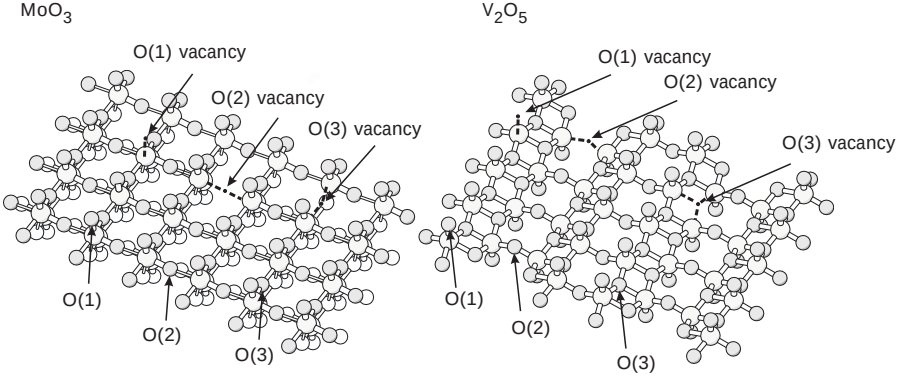

FIG. 2

Sketch of different surface oxygen sites O(1–3) and corresponding vacancies (black dots) at different surface oxygen sites of the MoO_3(010) and V_2O_5(010) surfaces

cally between two Mo centers of the surface layer (Mo–O distance 1.94 Å) and is only weakly linked to the third Mo center in the underlying sublayer (Mo–O distance 2.33 Å). In contrast, in V_2O_5 all three vanadium neighbors of O(3) lie at a similar V–O distance (1.78, 1.78 and 2.02 Å).

The existence of three structurally different oxygen centers at the surface allows for three types of oxygen vacancies (see Fig. 2), which can be annihilated by either oxygen diffusion from the bulk or atomic/molecular oxygen adsorption from gas phase. A complete re-oxidation cycle may be represented by a Triskel plot (Fig. 3). Starting from the undefected structure in the center, three types of vacancies, O(1), O(2), O(3), may be formed as a result of the catalytic reaction (*i.e.* hydrocarbon oxidation, formation and subsequent desorption of surface OH/H_2O groups, *etc.*). Oxygen vacancies may transform from one type to another by lattice diffusion. Further, an oxygen molecule from gas phase may be adsorbed at the vacancy and, through O–O bond dissociation followed by desorption of atomic oxygen, the initial undefected structure is restored. Prior to desorption, the oxygen may also undergo diffusion at the surface. Thus a three-armed spiral process network can be drawn, see Fig. 3, where the details of the network are rather complex. However, each part can be studied separately. In our previ-

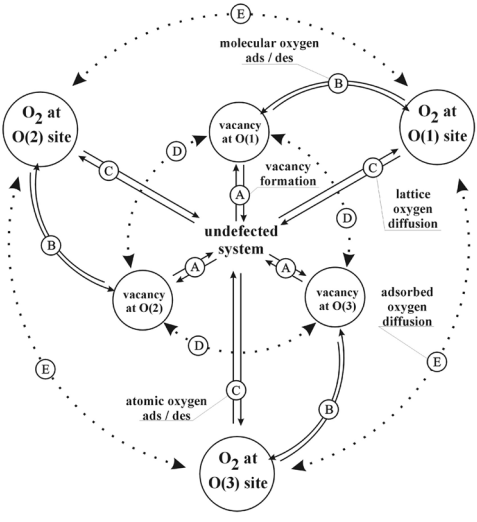

FIG. 3
Triskel plot representing a network of re-oxidation processes: path A, creation/annihilation of the given vacancy; path B, adsorption/desorption of O_2 molecule at/from the respective vacancy; path C, adsorption/desorption of oxygen atom at/from the cluster; path D, diffusion of vacancies at the surface; path E, diffusion of atomic oxygen at the surface

ous papers we investigated the formation of vacancies (paths A)[13–16] and their diffusion (paths D)[14]. Our present work focuses on the properties of molecular oxygen adsorbed at a vacancy (crossing points of paths B and C) and analyzes the consequences of surface re-oxidation. At this stage, the effect of adsorbed oxygen diffusion (path E) is not of primary interest.

In both oxides the (010) surfaces, which are the most interesting from a catalytic point of view, are modeled by large surface clusters cut out from the bulk, $Mo_{15}O_{56}$ and $V_{10}O_{31}$ sections. The clusters are bond saturated by hydrogen at their periphery leading to $Mo_{15}O_{56}H_{22}$ and $V_{10}O_{31}H_{10}$ cluster models, which have proven to represent electronic properties of the respective systems quite reliably[15]. Oxygen vacancies are described by removing oxygen from the three differently coordinated positions at the cluster surface while the filling of oxygen vacancies is simulated by adsorbing differently oriented oxygen molecules at the vacancy sites, O(1), O(2) or O(3). The surface clusters applied in this study form a reasonable balance between computational effort and accuracy as shown in test calculations using larger embedded clusters, such as $V_{16}O_{49}H_{18}$, $V_{20}O_{62}H_{24}$ (refs[15,17]) or $Mo_{20}O_{84}H_{48}$. In particular, chemical/physical parameters of oxygen vacancies at the MoO_3(010) surfaces, obtained form our cluster calculations, yield good agreement with recent periodic slab calculations[18].

COMPUTATIONAL

Electronic properties of the present systems are obtained from quantum chemical calculations using standard DFT methods[19,20]. Electronic exchange and correlations are accounted for by both local spin density (LSDA)[21] and gradient-corrected (GGA) functionals[22,23]. Further, Kohn–Sham orbitals are represented by linear combinations of atomic orbitals using extended basis sets of contracted Gaussian-type orbitals (CGTO). The basis sets for vanadium, oxygen, and hydrogen are all-electron type and of double zeta quality with additional polarization functions. For molybdenum an effective core potential is used to represent the [Ar]$3d^{10}$ core[24] while the valence basis is also of double zeta plus polarization quality. In all calculations, the DFT-LCGTO program package StoBe [25] is used. We emphasize that trying to increase the present orbital and fitting basis sets to very high quality size – as needed for small molecules in comparison with spectroscopy experiments of high accuracy – seems to be unnecessary. In the present surface study a microscopic understanding of physical/chemical behavior is much more relevant than numerical comparison with experimental data which may be rather inaccurate due to the complexity of the systems.

In all geometry optimizations of the present study the substrate cluster geometry is kept frozen whereas the centers of the O_2 adsorbate are allowed to relax. This procedure introduces errors due to the neglection of surface relaxation in response to the adsorbate. However, these errors are found to be of minor importance as shown in preliminary calculations for O_2 stabilization at an O(2) vacancy site of the V_2O_5(010) surface where a full geometry optimization of all surface atoms is included. Here the correction in the adsorption energy due to complete surface relaxation amounts to only 0.2 eV and V–O bond distances involving the adsorbed O_2 species are elongated by only 0.03 Å. The energy corrections are smaller than those of surface relaxation affecting oxygen vacancy formation which amount to 0.5 to 0.7 eV (ref.[15]) and are used to define an upper limit for the error in the O_2 adsorption energies. It is consistent with previous experience in cluster studies of H, H_2, and CO adsorption at V_2O_5(010) where local relaxation effects are found to yield similar corrections (see refs[14,15]). Thus, neglect of full surface relaxation will not change the discussion of the chemistry involved in the re-oxidation process described below.

While (partial) geometry optimizations are carried out using the computationally less expensive LSDA functional[21] total energies and electronic properties at the resulting equilibrium geometries are evaluated with the gradient-corrected RPBE functional[22,23] which has been found to yield quite accurate results in a number of surface studies, using both cluster[15] and periodic slab models[24]. Based on the RPBE results the electronic structure is characterized by Mulliken atomic charges[26], Mayer bond orders[27], density of states plots and maps of the electrostatic potential. The use of different functionals in the geometry optimization and in the final electronic structure evaluation leads to errors due to differences between LSDA and GGA derived equilibrium geometries. This has been tested for the present V_2O_5(010) clusters and yields differences in atom positions below 0.05 Å (ref.[28]) translating to errors in the O_2 adsorption energy of the order 0.1 eV at most, well within the error bar of the present model approximations. The error can thus be neglected in the present discussion.

RESULTS AND DISCUSSION

Energetics

The re-oxidation process requires oxygen vacancies to be present at the oxide surface (vacancy formation has been described in detail previously[13–16]). The mechanism of this process depends strongly on the reaction under

consideration and, therefore, cannot be discussed in general. However, for each catalyst characteristic energies describing binding properties of lattice oxygen as well as of oxygen filling of the corresponding vacancies can be defined. In the present work the discussion is limited to initial and final state energetics of re-oxidation while keeping in mind that transition states connected with energy barriers play an important role in an account of specific reaction paths.

The energy of vacancy formation E_D is defined as the difference between the sum of energies of the products (*i.e.* a defected oxide cluster – with one oxygen atom missing – and a free oxygen atom) and the energy of the substrate (an "undefected" oxide cluster), *i.e.*

$$E_D = E(M_mO_{n-1}H_k) + E(O) - E(M_mO_nH_k)\,, \qquad (1)$$

where $M_mO_nH_k$ = $Mo_{15}O_{56}H_{22}$, $V_{10}O_{31}H_{12}$ for MoO_3, V_2O_5, respectively. Thus the (positive) E_D values describe removal energies of neutral oxygen species from the surface and represent an upper limit for vacancy formation energies neglecting possible desorption barriers. The computed (rather large) vacancy energies E_D listed in Table I for both MoO_3 and V_2O_5 demonstrate that the lattice oxygen is always very strongly bound at the surface.

TABLE I

Energies of vacancy formation E_D, molecular oxygen adsorption at a vacancy $E_B(O_2)$ and atomic oxygen adsorption at the surface $E_B(O)$ for surface sites O(1), O(2), O(3) at the MoO_3(010) and V_2O_5(010) surfaces using $Mo_{15}O_{56}H_{22}$ and $V_{10}O_{31}H_{12}$ clusters, respectively. All energies are given in eV

Energy	O(1) parallel/perpendicular	O(2) parallel/perpendicular	O(3) "parallel"
MoO_3			
E_D	6.80	6.75	6.50
$E_B(O_2)$	–2.98/–2.39	–1.11/–	–0.08
$E_B(O)$	–1.77/–1.19	–0.02/–	0.82
V_2O_5			
E_D	7.16	7.95	7.01
$E_B(O_2)$	–2.53/–2.16	–3.27/–2.76	–1.03
$E_B(O)$	–1.50/–1.13	–1.38/–0.87	0.05

The vacancy energy E_D is larger for V_2O_5 (7–8 eV) than for MoO_3 (6.5–7 eV). This energy can be decreased by adsorption of hydrogen atom(s) and creation of surface hydroxyl or water species which may be easily desorbed, as was shown previously[13].

In a subsequent step oxygen vacancies may be annihilated by oxygen diffusing from the bulk (vacancy diffusion into the bulk) or filled by the adsorption of oxygen molecules from gas phase. In the latter process, molecular oxygen adsorbs at different vacancies (O(1), O(2), O(3)) and with different geometric orientation (*e.g.* perpendicular or parallel to the surface). Adsorbate geometries obtained from the present calculations are shown in Fig. 4.

Table I contains also the energies associated with the adsorption of molecular oxygen at different oxygen vacancy sites of the MoO_3 and V_2O_5 surfaces. Here the adsorption energy of molecular oxygen, $E_B(O_2)$, is defined as the difference between the energy of the adsorbate system (a defected cluster with an oxygen molecule adsorbed at a vacancy) and the sum of the energies of the defected cluster and a free oxygen molecule, *i.e.*

$$E_B(O_2) = E(M_mO_{n-1}H_kO_2) - [E(M_mO_{n-1}H_k) + E(O_2)] , \qquad (2)$$

where $M_mO_nH_k$ = $Mo_{15}O_{56}H_{22}$, $V_{10}O_{31}H_{12}$ for MoO_3, V_2O_5, respectively. Negative $E_B(O_2)$ values of the binding energy indicate that adsorption is an exothermic, favorable process.

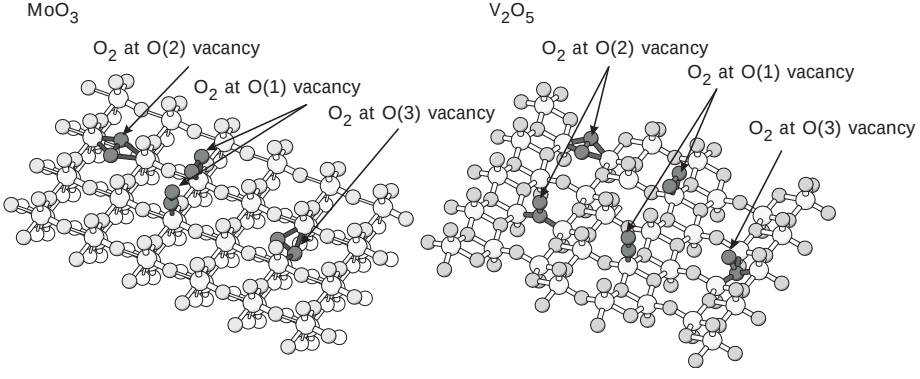

FIG. 4
Sketch of computed equilibrium geometries of an adsorbed O_2 molecule at different vacancy sites of the MoO_3(010) and V_2O_5(010) surfaces. The results are obtained by optimizing the O_2 position and geometry in the $Mo_{15}O_{55}H_{22}$ and $V_{10}O_{30}H_{12}$ vacancy cluster models. The O_2 adsorbate species are shown by shaded balls while the surface lattice is sketched by lighter balls

For MoO_3 the most stable adsorption of molecular oxygen is found at the O(1) vacancy site ($E_B(O_2)$ = –2.98 eV). Adsorption at an O(2) vacancy is considerably less favored ($E_B(O_2)$ = –1.11 eV) while negligible stabilization ($E_B(O_2)$ = –0.08 eV) is found at an O(3) vacancy site. This ordering goes in parallel with the energies of vacancy formation (see Table I) – the oxygen molecule is favorably adsorbed at vacancies with high formation energy. However, the interesting point is that despite almost identical energies of the O(1) and O(2) vacancy formation (6.80 and 6.75 eV, respectively) the adsorption of molecular oxygen at the O(1) vacancy is strongly favored (–2.98 eV in contrast to –1.11 eV for O(2)). In addition, the O(1) vacancy is the only site where perpendicular adsorption of O_2 is possible (referring to a local energy minimum). For all other vacancies only parallel adsorption is observed. Further, adsorption at the O(1) vacancy is energetically favored over adsorption at any other site – probably due to the lack of sterical hindering. In the case of adsorption at the O(2) vacancy all starting geometries lead to an O_2 orientation parallel to the surface (Fig. 4). The O_2 molecule adsorbed at the O(3) vacancies is pulled towards the bulk and the resulting orientation is an intermediate between parallel and perpendicular (see Fig. 4) orientation.

In the case of V_2O_5, molecular oxygen is most stable at the O(2) vacancy ($E_B(O_2)$ = –3.27 eV), less stable at O(1) ($E_B(O_2)$ = –2.53 eV) and is the least stable at O(3) ($E_B(O_2)$ = –1.03 eV). Similarly to MoO_3, this trend is consistent with the order of energies needed to create a vacancy: replenishing the O(2) vacancy by molecular oxygen leads to the largest decrease in total energy of the system while annihilation of an O(3) vacancy releases much less energy. Analogous to MoO_3, re-oxidation of the O(3) vacancy by O_2 yields the intermediate orientation (between parallel and perpendicular) and the oxygen molecule is also incorporated into the surface. For other vacancies, parallel adsorption of O_2 is preferred over perpendicular. However, the "site" trend is stronger than the "orientation" trend, *i.e.*, both orientations (parallel and perpendicular) at the O(1) vacancy possess lower $E_B(O_2)$ than any orientation at O(2) vacancy (see Table I).

In order to restore the initial state (an undefected cluster) one oxygen atom must be removed after the O_2 molecule is adsorbed at the vacancy. In analogy to the adsorption energy of molecular oxygen, the energy of atomic oxygen adsorption, $E_B(O)$, can be defined by

$$E_B(O) = E(M_mO_nH_kO) - [E(M_mO_nH_k) + E(O)] , \qquad (3)$$

where $M_mO_nH_k$ = $Mo_{15}O_{56}H_{22}$, $V_{10}O_{31}H_{12}$ for MoO_3, V_2O_5, respectively.

For both systems, the removal of an oxygen atom from the O_2 molecule adsorbed at an O(3) vacancy is spontaneous (positive value of E_B(O), see Table I). In contrast, bond splitting of the O_2 adsorbate at the other vacancies requires energy, up to 1.77 eV. Moreover, for MoO_3 the above process occurring at an O(2) vacancy costs almost no energy (E_B(O) = –0.02 eV). Small, negative E_B(O) values describing the removal of oxygen atom from the O_2 adsorbate indicate the presence of easily released active oxygen atom. One should stress that in the case of oxygen adsorption at O(3) vacancy the E_B(O) values are even positive. Therefore this atom can be proposed as the electrophilic surface oxygen species responsible for total oxidation of hydrocarbons.

Discussing the reaction energetics one should keep in mind that reaction rates always depend on corresponding energy barriers, which in turn depend on the specific reactant used and cannot be determined by considering the catalyst surface only. Knowing that the energy barrier can never be smaller than the energy difference between products and substrates, small E_B(O) values indicate that, in favorable circumstances, the barrier may also be small.

Mulliken Charges and Mayer Bond Orders

Adsorption of molecular oxygen at a surface oxygen vacancy can be viewed as replacing a lattice oxygen atom by an O_2 molecule. This observation is strongly supported by the analysis of Mulliken charges (Table II) and Mayer bond orders describing bonds between adsorbed O_2 and its vanadium neighbors (Table III). To make the discussion easier, the two atoms of the O_2 molecule are distinguished by denoting them as O_a and O_b for the atom closer and further from the surface, respectively. In the case of parallel adsorption both oxygen atoms are equivalent.

The total charge of the O_2 molecule at the oxygen vacancy is very close to that of the lattice oxygen atom occupying the corresponding site at the undefected surface. In the case of MoO_3 the total charge of O_2 adsorbed at the O(1) vacancy is equal to –0.50, compared to the charge of an O(1) atom in the undefected cluster, which is –0.48. The sum of charges of the two adsorbed oxygen atoms of O_2 at the O(3) vacancy is found to be equal to –1.02 while in cluster the O(3) atom has a charge of –1.00. Only for the O(2) vacancy the difference between the O_2 charge and that of corresponding lattice oxygen at the surface is slightly larger (0.09 e). The same tendency is found for V_2O_5. Here also the charges characterizing the adsorbed

O_2 molecule are very close to those of the lattice oxygen occupying respective sites on the undefected surface.

The above results lead to the conclusion that mostly its crystallographic environment determines the charge at a specific lattice site at the surface. In effect, the charge characteristic of the lattice oxygen is redistributed (equally in the case of parallel orientation) between the two oxygen atoms of adsorbed O_2 at the respective site. This means that adsorbed molecular oxygen can replace a surface oxygen atom occupying a specific lattice site with almost no change in electron distribution in the crystallographic neighborhood.

Upon adsorption at the vacancy site the oxygen molecule becomes activated. Its O–O bond elongates and the corresponding bond order decreases (see Table III). For all geometries considered in this work the O_2 activation is stronger for parallel than for perpendicular orientation. The O_2 bond length increases from 1.24 Å in gas phase to 1.49 Å for MoO_3 and up to 1.47 Å for V_2O_5. The largest elongation is found for adsorption of O_2 at vacancies formed at highly coordinated oxygen sites, O(3). Bond lengths obtained for parallel adsorption are comparable with the calculated bond

TABLE II

Selected atom charges $Q(O_{a/b})$ (from Mulliken population analysis) of the adsorbed oxygen molecule at O(1), O(2), and O(3) vacancies of the $Mo_{15}O_{56}H_{22}$ and $V_{10}O_{31}H_{12}$ clusters representing MoO_3(010) and V_2O_5(010) surfaces. In addition, atom charges $Q(O_{cluster})$ for lattice oxygen present at the corresponding vacancy site on the undefected surface are included in the Table

Atom charge	O(1) parallel/perpendicular	O(2) parallel/perpendicular	O(3) "parallel"
MoO_3			
$Q(O_{cluster})$	–0.48	–0.73	–1.00
$Q(O_a)$	–0.25/–0.20	–0.41/–	–0.58
$Q(O_b)$	–0.25/–0.22	–0.41/–	–0.44
V_2O_5			
$Q(O_{cluster})$	–0.33	–0.69	–0.87
$Q(O_a)$	–0.18/–0.14	–0.30/–0.46	–0.50
$Q(O_b)$	–0.18/–0.18	–0.30/–0.26	–0.35

length in isolated O_2^- species (1.39 Å). Increasing the bond length in the adsorbed oxygen molecule leads to a weakening of its O–O bond. In contrast to the bond order characteristic of a free O_2 molecule (equal to 1.87), which indicates almost a double bond, bond orders between 0.8 and 0.9 are found for adsorbed O_2 at MoO_3 and close to 0.9 for V_2O_5, indicating single O–O bonds in all cases. For perpendicular adsorption of the O_2 molecule its bond lengths remain almost unchanged compared with the free molecule (1.25 Å for MoO_3, 1.25 and 1.33 Å for V_2O_5). However, the bond orders (1.08 Å for MoO_3, 1.19 and 1.07 Å for V_2O_5) indicate bond weakening.

TABLE III

Selected distances and bond orders (in parentheses) of the $Mo_{15}O_{56}H_{22}$ and $V_{10}O_{31}H_{12}$ clusters representing MoO_3(010) and V_2O_5(010) surfaces with an oxygen molecule adsorbed at O(1–3) vacancies. All bond lengths are given in Å

Bond	O(1) parallel/perpendicular	O(2) prallel/perpendicular	O(3) "parallel"
MoO_3			
O_a–O_b	1.41(0.93)/1.25(1.08)	1.45(0.87)/–	1.49(0.79)
Mo–O_a	1.92(0.89)/1.80(0.72)	1.89(0.55)/–	2.06(0.20)
		2.33(0.15)/–	2.05(0.32)
			2.16(0.10)
Mo–O_b	1.92(0.89)/3.04(0.73)	1.89(0.55)/–	2.10(0.26)
		2.33(0.15)/–	2.13(0.31)
			2.73(0.02)
V_2O_5			
O_a–O_b	1.38(0.95)/1.25(1.19)	1.41(0.90)/1.33(1.07)	1.47(0.84)
V–O_a	1.79(1.02)/1.65(1.06)	1.96(0.48)/1.83(0.48)	1.91(0.31)
		1.96(0.48)/1.83(0.48)	1.99(0.29)
			1.91(0.33)
V–O_b	1.78(1.03)/2.91(0.70)	1.96(0.48)/2.61(0.28)	2.15(0.27)
		1.96(0.48)/2.61(0.28)	2.26(0.19)
			2.16(0.26)

Considering the adsorbed O_2 molecule as two oxygen atoms at the surface (which applies especially to parallel orientation where the O_2 molecule is activated) one may conclude that re-oxidation proceeding through gaseous oxygen provides more electrophilic surface oxygen (defined by Mulliken charges) as compared to the clean, undefected surface.

Densities of States

Additional information about changes in reactivity at the oxide surface resulting from vacancy filling by molecular gaseous oxygen can be obtained from atom-projected, partial densities of states (PDOS). Figure 5 presents atom-projected densities of states for both MoO_3 and V_2O_5 systems. Each plot shows contributions from two atoms (O_a, O_b) of the adsorbed O_2 molecule (lower part) and compares them with the density of a corresponding oxygen center in the undefected cluster (upper part). For parallel orientation at O(1) and O(2) vacancies both atoms are equivalent and hence give exactly the same PDOS contributions. For O(3) vacancies, where an intermediate orientation between parallel and perpendicular is found, the contributions from non-equivalent O_a and O_b atoms are plotted.

In general, replacing the lattice oxygen by an O_2 molecule results in a shift of oxygen levels towards the HOMO region. This means that the orbitals originating from the adsorbed oxygen molecule take part in the chemically active molecular orbital (HOMO). For adsorption at an O(3) vacancy (for both systems), where the atoms of the adsorbed oxygen molecule are non-equivalent, the atom located farther from the surface exhibits a higher contribution to the valence region, which suggests a higher activity compared to that of the other oxygen atom.

Electrostatic Potential Maps

The topography of the electrostatic potential (EP) above the catalyst surface can determine how an approaching molecule will orient itself at particular adsorption sites. Figures 6 and 7 compare EP maps of the undefected surface clusters with those where an oxygen molecule adsorbs at different vacancy sites for MoO_3 and V_2O_5, respectively. Adsorption of an O_2 molecule at an O(1) vacancy distorts the EP about the adsorption site considerably. For both systems under consideration the potentials are characterized by less negative values and assume the form of relatively wide and shallow basins. Adsorption at other vacancy sites proceeds differently for the two

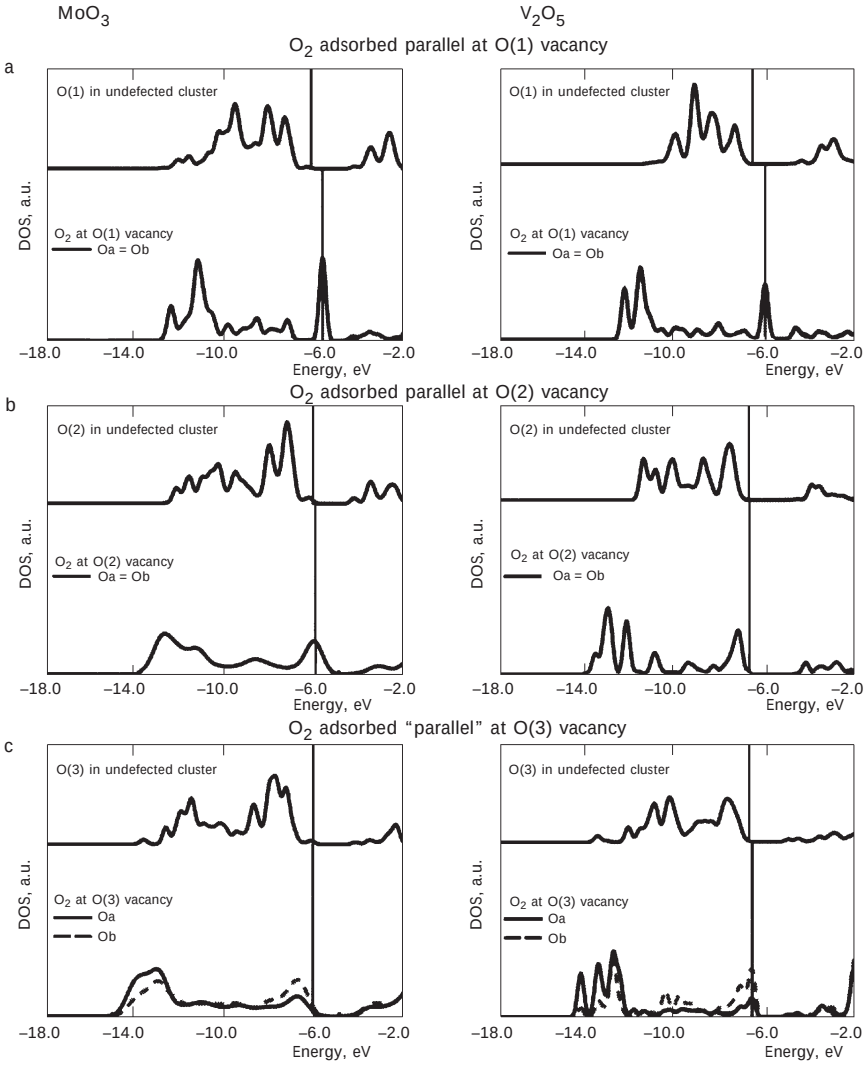

FIG. 5

Atom-projected PDOS curves of the valence band region for the $Mo_{15}O_{55}H_{22}$ and $V_{10}O_{30}H_{12}$ clusters. Each plot consists of two parts: lower, PDOS corresponding to two oxygen atoms of O_2 molecule adsorbed at a given vacancy; upper, PDOS for the lattice oxygen occupying the respective vacancy site at the undefected surface. A Gaussian level broadening of 1 eV is applied and the energetic position of the HOMO is marked by a vertical line. a Parallel adsorption of O_2 at O(1) vacancy, identical contributions from oxygen O_a, O_b; b parallel adsorption of O_2 at O(2) vacancy, identical contributions from oxygen O_a, O_b; c nearly parallel adsorption of O_2 at O(3) vacancy, contributions from oxygen O_a, O_b are different due to asymmetric adsorption

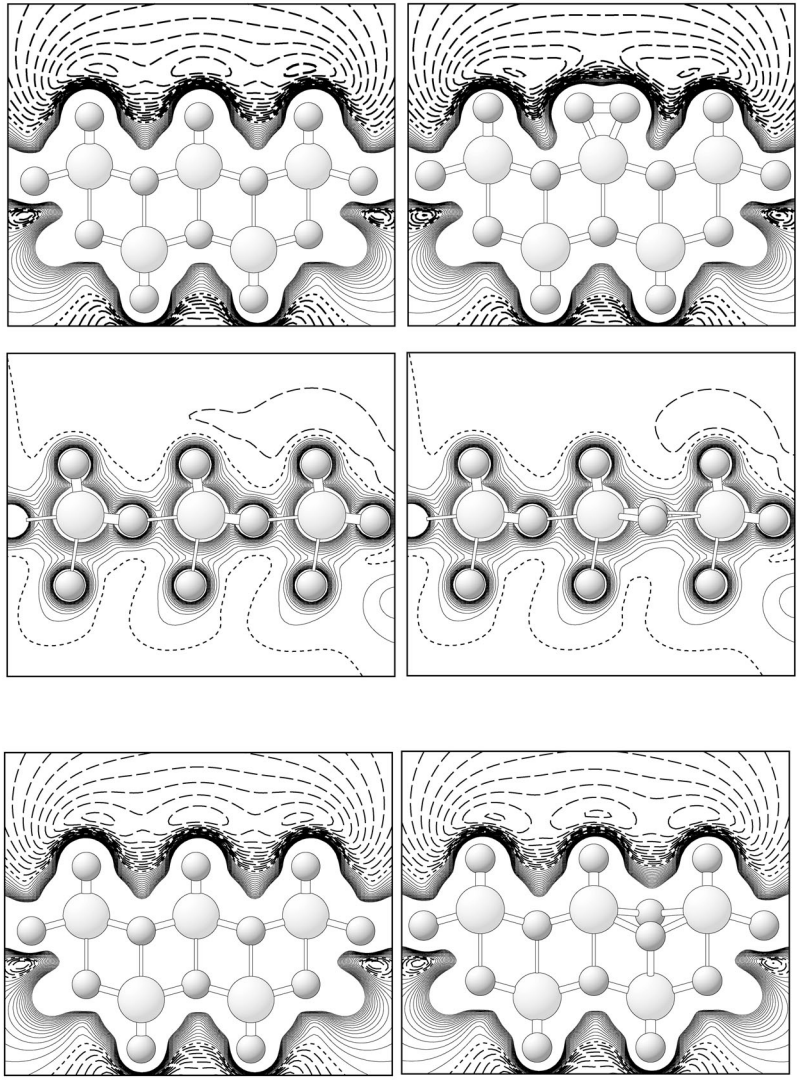

FIG. 6

Contour plots of the electrostatic potential about the $MoO_3(010)$ surface for a $Mo_{15}O_{56}H_{22}$ cluster. The contours are shown for planar sections perpendicular to the surface. Contour values refer to increments of 0.02 eV with positive (negative) values given by solid (long-dashed) lines. Zero lines are shown with small dashes. The left/right plots describe undefected clusters and clusters with an adsorbed O_2 molecule, respectively, shown for the same planar section. The plots refer to O_2 adsorbed near the O(1) vacancy (top row), near the O(2) vacancy (middle row, note that the second substrate layer of atoms does not show due to its off-plane position), near the O(3) vacancy (bottom row)

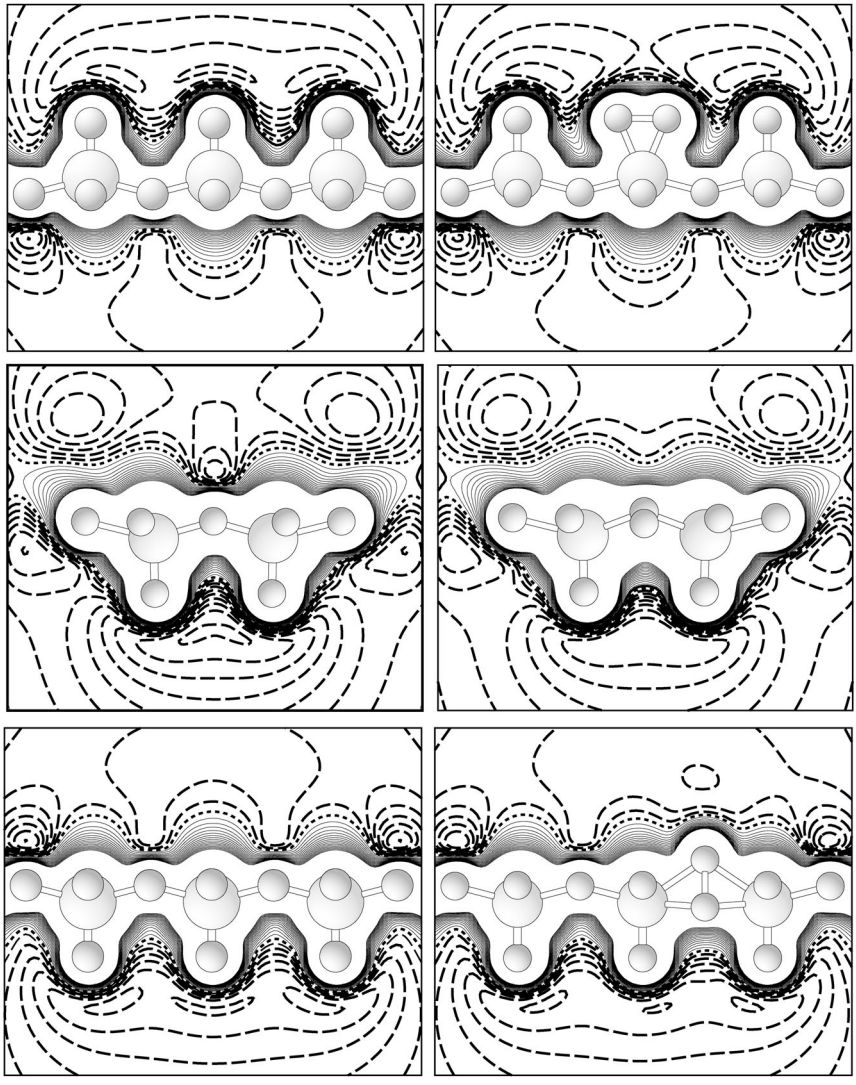

FIG. 7

Contour plots of the electrostatic potential about the $V_2O_5(010)$ surface for a $V_{10}O_{31}H_{12}$ cluster. The contours are shown for planar sections perpendicular to the surface. Contour values refer to increments of 0.02 eV with positive (negative) values given by solid (long-dashed) lines. Zero lines are shown with small dashes. The left/right plots describe undefected clusters and clusters with an adsorbed O_2 molecule, respectively, shown for the same planar section. The plots refer to O_2 adsorbed near the O(1) vacancy (top row), near the O(2) vacancy (middle row), near the O(3) vacancy (bottom row)

systems, MoO_3 and V_2O_5. For MoO_3 molecular O_2 adsorption at O(2) and O(3) vacancies leads to negligible changes in the electrostatic potential. This may be explained by the topography of the MoO_3(010) surface which is densely covered by molybdenyl groups influencing the electrostatic potential. In the case of V_2O_5 adsorption of molecular O_2 at both O(2) and O(3) vacancies results in more pronounced changes. Here the deep basin of negative potential present above the O(2) site in the undefected cluster disappears after the oxygen molecule is adsorbed. This contrasts with the adsorption at the O(3) vacancy where, apart from breaking the symmetry of the potential, an additional local minimum appears above the adsorbed oxygen molecule.

CONCLUSIONS

The present study shows that the re-oxidation proceeding *via* molecular oxygen adsorption is a very localized process. For both systems, MoO_3 and V_2O_5, the energies needed to form vacancies, E_D, are of the order 7–8 eV indicating very strong bonding of surface oxygen. The process of vacancy formation, can, however, be facilitated by adsorption of hydrogen resulting in surface hydroxyl or water species, which may be easily desorbed.

A possible way to re-oxidize the surface is to fill oxygen vacancies by gaseous (molecular) oxygen. Molecular oxygen adsorbs at any surface vacancy with energies $E_B(O_2)$ depending on the specific site where the calculations yield the order O(1) < O(2) < O(3) vacancies for MoO_3 and O(2) < O(1) < O(3) vacancies for V_2O_5. For all sites parallel O_2 adsorption is preferred over perpendicular. Oxygen molecules adsorbed at given vacancies assume charges similar to those of the corresponding lattice oxygen at undefected surface. This means that adsorbed molecular oxygen can replace the surface oxygen occupying a specific lattice site with almost no change in the electron distribution of the crystallographic neighborhood. Thus, the oxide surface is able to incorporate large amounts of (weakly bound) oxygen atoms. The charge characteristic of the lattice oxygen is redistributed between the two oxygen atoms of the O_2 adsorbate providing more electrophilic surface oxygen (defined by Mulliken charges) as compared to the clean, undefected surface.

Replacing the lattice oxygen by O_2 molecules results in a shift of oxygen levels towards the HOMO region. Thus, the orbitals originating from the adsorbed oxygen molecule take part in the chemically active molecular orbital (HOMO). Further, the oxygen molecule becomes activated by adsorption at the vacancy site. Its O–O bond elongates and the corresponding

bond order decreases. For all studied geometries the O_2 activation is always stronger for parallel than for perpendicular orientation.

The activated oxygen molecule can undergo dissociation. Small, negative values of energies, describing the removal of an oxygen atom from the O_2 adsorbate, indicate the presence of active oxygen that can be easily released. This oxygen is proposed as the electrophilic surface oxygen species responsible for total oxidation of hydrocarbons.

Discussing the re-oxidation process one should keep in mind that reaction rates always depend on corresponding energy barriers, which in turn depend on the specific reactant used and cannot be determined by considering the catalyst surface only. Another important factor to be taken into account is the full geometry optimization of the reaction system. Such studies are presently under way.

This work was funded in parts by grant No. 7 T09A 119 21 from the State Committee for Scientific Research of Poland.

REFERENCES

1. Grzybowska-Świerkosz B.: *Appl. Catal. A* **1997**, *157*, 263.
2. Bielanski A., Haber J.: *Oxygen in Catalysis*. Marcel Dekker Inc., New York 1991.
3. a) Che M., Tench A. J.: *Adv. Catal.* **1982**, *31*, 78; b) Che M., Tench A. J.: *Adv. Catal.* **1983**, *32*, 1.
4. Haber J., Turek W.: *J. Catal.* **2000**, *190*, 320.
5. Braithwaite E. R., Haber J. (Eds): *Molybdenum: An Outline of Its Chemistry and Uses, Studies in Inorganic Chemistry*, Vol. 19. Elsevier, Amsterdam 1994.
6. Kung H. H. in: *Studies in Surface Science and Catalysis* (B. Delmon and J. T. Yates, Eds), Vol. 45. Elsevier, Amsterdam 1989.
7. Mestl G., Srinivasan T. K. K.: *Catal. Rev.–Sci. Eng.* **1998**, *40(4)*, 451.
8. Henrich V. E., Cox P. A.: *The Surface Science of Metal Oxides*. University Press, Cambridge 1994.
9. Kihlborg L.: *Acta Chem. Scand.* **1969**, *23*, 1834.
10. Ekstrom T., Nygren M.: *Acta Chem. Scand.* **1972**, *26*, 1827.
11. Bystrom A., Wilhelmi K. A., Brotzen O.: *Acta Chem. Scand.* **1950**, *4*, 1119.
12. Bachmann H. G., Ahmed F. R., Barnes W. H.: *Z. Kristallogr.* **1961**, *115*, 110.
13. Hermann K., Witko M., Druzinic R., Tokarz R.: *Top. Catal.* **2000**, *11/12*, 67.
14. Hermann K., Witko M., Druzinic R., Tokarz R.: *Appl. Phys. A: Solids Surf.* **2001**, *72*, 429.
15. Hermann K., Witko M. in: *Oxide Surfaces* (D. P. Woodruff, Ed.), p. 136. Elsevier, Amsterdam 2001.
16. Tokarz-Sobieraj R., Hermann K., Witko M., Blume A., Mestl G., Schloegl R.: *Surf. Sci.* **2001**, *489*, 107.

17. Witko M., Hermann K., Tokarz R., Druzinic R., Chakrabarti A. in: *Metal Ligand Interactions in Chemistry, Physics, and Biology* (N. Russo and D. Salahub, Eds), NATO Science Series C, Vol. 546, p. 417. Kluwer, Dordrecht 2000.
18. Chen X., Friend X., Kaxiras X.: *J. Am. Chem. Soc.* **2001**, *123*, 2224.
19. Labanowski J. K., Andzelm J. W. (Eds): *Density Functional Methods in Chemistry*. Springer-Verlag, New York 1991.
20. Godbout N., Salahub D. R., Andzelm J. W, Wimmer E.: *Can. J. Phys*. **1992**, *70*, 560.
21. Vosko S. H., Wilk L., Nusair M.: *Can. J. Phys*. **1980**, *58*, 1200.
22. Perdew J. P., Burke K., Ernzerhof M.: *Phys. Rev. Lett*. **1996**, *77*, 3865.
23. Hammer B., Hansen L. B., Norskov J. K.: *Phys. Rev. B: Condens. Matter* **1999**, *59*, 7413.
24. Andzelm J., Radzio E., Salahub D. R.: *J. Chem. Phys*. **1985**, *83*, 4573.
25. The program package StoBe is a modified version of the DFT-LCGTO program package DeMon, originally developed by A. St.-Amant and D. Salahub (University of Montreal), with extensions by L. G. M. Petterson and K. Hermann.
26. a) Mulliken R. S.: *J. Chem. Phys*. **1955**, *23*, 1833; b) Mulliken R. S.: *J. Chem. Phys*. **1955**, *23*, 1841; c) Mulliken R. S.: *J. Chem. Phys*. **1955**, *23*, 2388; d) Mulliken R. S.: *J. Chem. Phys*. **1955**, *23*, 2343.
27. Mayer I.: *J. Mol. Struct. (THEOCHEM)* **1987**, *149*, 81.
28. Druzinic R.: *Ph.D. Thesis*. Free University, Berlin 2000.